Spreading profile of evaporative liquid drops in thin porous layer

W. Y. Chong,[1,*] K. S. Lim,[1] W. H. Lim,[1] S. W. Harun,[1,2] F. R. Mahamd Adikan,[1,2] and H. Ahmad[1]
[1]*Photonic Research Centre, Department of Physics, Faculty of Science, University of Malaya, 50603 Kuala Lumpur, Malaysia*
[2]*Department of Electrical Engineering, Faculty of Engineering, University of Malaya, 50603 Kuala Lumpur, Malaysia*
(Received 13 May 2011; revised manuscript received 13 October 2011; published 19 January 2012; corrected 22 May 2012)

Spreading of evaporative liquid drops in a thin porous layer has been studied. The entire spreading process can be divided into three distinct phases according to the change of the wetted porous region size. The first phase is characterized by the expansion of the wetted porous region and shrinking of the liquid drop. Contact line pinning is observed in the wetted porous region in the second phase even with the liquid drop totally absorbed into the porous layer. The third phase sees the shrinkage of the wetted porous region until it is not observable. Based on these observations, a model is devised to simulate the spreading of a liquid drop under the studied conditions. Partial differential equations are used to describe the relation between liquid drop volume and other important parameters of a fluid flow, including maximum wetted region diameter achieved, time taken to reach each spreading process phase, and evaporation rate. Calculated results are in good agreement with the experimental data.

DOI: 10.1103/PhysRevE.85.016314 PACS number(s): 47.56.+r, 64.70.fm

I. INTRODUCTION

Many applications involving liquid drop adhesion, such as spray coating, painting, and ink jet printing, involve liquid contact not with a homogeneous flat surface but with a thin porous layer. Concurrence of infiltration, redistribution, and evaporation of a liquid drop in a thin porous layer is a common phenomenon observed for water balance in natural porous media. Therefore, it is important to understand fluid flow within a liquid drop as well as in the porous layer, which in turn determines the distribution of solid particles within the liquid drop after the drying process. Fluid flow within an evaporating liquid drop on a solid surface can be ascribed to contact line pinning of the liquid drop due to capillary flow of liquid from the interior to the periphery of the drop to compensate for higher evaporation rate at the periphery [1,2]. This effect results in solute accumulation at the periphery of a liquid drop after drying, popularly termed the "coffee-ring" effect. The study was then developed to consider imbibitions of a liquid drop into a porous media and the fluid flow within. This has prompted studies of fluid flow in such realistic conditions. Starov *et al*. have been major contributors in the studies of fluid flow in porous layer and have considered nonevaporative liquid drop spreading in both a porous layer saturated with the same liquid and later in a dry porous layer [3,4]. Spreading of an aqueous liquid drop on porous layers has later been studied by considering drop volume conservation during the spreading process [5,6].

Evaporation of liquid from thick porous slabs of the same as well as different porosity has been reported by Shokri *et al*. [7,8] and Bechtold *et al*. [9]. It is found that evaporation from a thick porous layer, namely a sand column, involves continuous capillary flow of liquid from wetted zones below the surface [10].

This work studies fluid flow of an evaporative liquid drop in a thin porous layer. Experimental work has been performed to observe spread dynamics of an aqueous liquid drop on a thin porous layer. Based on observation, an analytical solution of liquid drop spreading on a thin porous layer with consideration of liquid evaporation is postulated. It is found that the analytical result agrees very well with experimental observation.

This paper is arranged in seven sections. A description of the experimental setup used to observe liquid drop spreading is presented in Sec. II. Preliminary observation of liquid flow in a porous layer is discussed in Sec. III. From the observation, the principle of evaporative fluid flow in a thin porous layer is proposed in Sec. IV. Section V discusses an analytical solution of fluid flow according to the proposed principles. Comparison of experimental results with the predictions of the model discussed in Sec. V is presented in Sec. VI. Conclusion of this work is made in Sec. VII.

II. EXPERIMENTAL SETUP

The experimental setup for this work is shown in Fig. 1. De-ionized (DI) water was used as the liquid drop as it is a common solvent for many inorganic chemicals. The use of DI water also allows a straightforward relation between liquid weight and volume, where 1 g of DI water has a volume of 1 cm^3. A drop of DI water with known volume was applied on a thin porous layer using a micropipette. The porous layer used is a heat-treated silica soot layer deposited on silicon wafer via flame hydrolysis deposition. The porous layer thickness Δ is 25 ± 1 μm with porosity of $75 \pm 5\%$ and an average pore size of 2 μm.

Evolution of the liquid drop and spreading of the wetted porous region was recorded using a CCD camera capturing images from the side and top position, respectively. The evaporation of DI water was monitored by measuring the change in weight of the sample at time intervals of 5 s throughout the spreading, using a digital analytical balance with 0.1 mg precision. Focus was given to the spreading of the wetted porous region as the evolution of a water drop spreading on a solid surface is well established. The measurements were done in a clean room where the ambient temperature

*wuyi80@yahoo.com

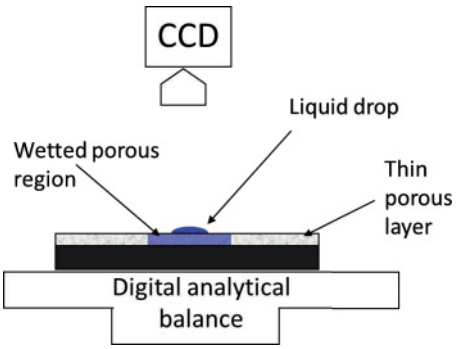

FIG. 1. (Color online) Experimental setup to measure the spread diameter of the wetted porous region and the weight of the remaining liquid solvent in a thin porous layer. For measurement of the liquid drop profile, the CCD camera is repositioned to capture images from the side. The porous layer thickness, Δ is 25 ± 1 μm with average pore size of 2 μm (CCD: charge-coupled device).

and relative humidity were controlled at (25 ± 1) °C and 55%–60%, respectively.

III. PRELIMINARY OBSERVATION

Figure 2 shows the spreading of the wetted porous region at different progressive times after application of DI water drop. The DI water volume applied, in this case, was 3.9 μl. The liquid-containing soot layer—wetted porous region—shows a darker color compared to the surrounding dry soot layer. The darker color is believed to be the color of the silicon substrate as the replacement of air refractive index (RI) of 1.0 with higher refractive index liquid ($RI_{water} = 1.33$) in the pores makes the wetted porous layer more "transparent" [11]. Thus the color intensity of the wetted porous region allows qualitative comparison of the liquid-filled pore fraction within the wetted porous region.

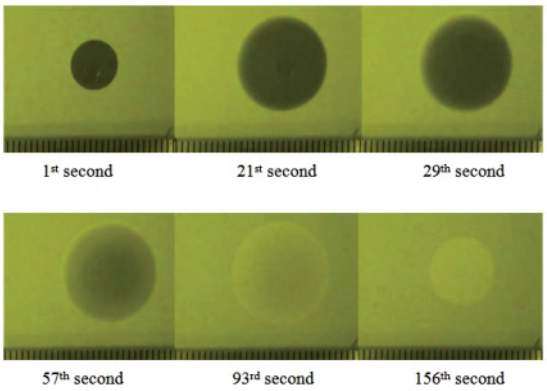

FIG. 2. (Color) Observation of liquid drop and wetted porous region size over time. Liquid drop volume used is 3.9 μl. Three distinct phases were observed. The first phase corresponds to the spreading of DI water upon application of a water drop (first second) to the complete formation of the wetted porous region (29th second). The second phase corresponds to the "pinning" of wetted porous region with changing color intensity over time as observed between the 29th and 57th seconds. The third phase corresponds to the shrinking of the wetted porous region (starts at 135th second) until it disappears at the 263th second. Scale division is 1 mm.

The white ring was believed to be the region with lower liquid-filled pore fraction as a result of higher evaporation rate at the wetted porous region boundary. The conservation of the wetted porous region boundary is a known phenomenon of liquid compensation from the body of the wetted porous region termed "contact line pinning." It is interesting to note that contact line pinning in this case occurs in the porous layer instead of on the surface. The supply of liquid from the body to the boundary of the wetted porous region is believed to be due to Darcy's fluid flow in porous structures in the direction of reducing capillary pressure. At the same time, the wetted porous region was observed to experience a bleaching effect where its color gradually changed from dark to white, as shown at the 57th second and the 93rd second. When the color of the wetted porous region body matched that of the ring boundary, it then shrank inward (156th second) and eventually disappeared. The total spreading process time is 263 s. The total time taken is about five times shorter compared to the time taken for total evaporation of a liquid drop from a solid surface [2].

IV. PRINCIPLE OF EVAPORATIVE FLUID FLOW IN A THIN POROUS LAYER

From the observation above, when an evaporative liquid drop is applied onto a porous layer, spreading of liquid in the thin porous layer can be divided into three phases as described below:

A. First phase

The first phase of liquid spreading in a thin porous layer is the wetted porous region formation. It is initiated upon contact of a volume of liquid with the porous layer. The first phase is characterized by the shrinkage of the liquid drop on the porous layer surface and the corresponding expansion of the wetted porous region, and can be represented by the illustration in Fig. 3(a). These processes were first reported by Starov *et al.* [3,4].

When an aqueous liquid drop is applied onto the surface of a porous layer, the liquid drop exhibits an axisymmetry profile, resembling a typical spherical shape as observed when a drop is formed on a solid surface. The liquid drop base was observed to reach maximum radius almost instantaneously.

Instead of maintaining its base area throughout the spreading process, the drop shrinks at a relatively fast rate through imbibitions of its volume into the porous layer. When the porous layer surrounding the liquid drop is saturated, the liquid then flows in the outward direction into the unsaturated soot layer, resulting in the expansion of the wetted porous region. Both shrinkage of the liquid drop and expansion of the wetted porous region occur simultaneously. Therefore, the expansion rate of the wetted porous region is related to the liquid drop volume. The total imbibition of liquid drop volume into the porous layer results in the halt of wetted porous region expansion.

B. Second phase

The expansion halt of the wetted porous region indicates the end of the first phase of liquid drop spreading and the onset

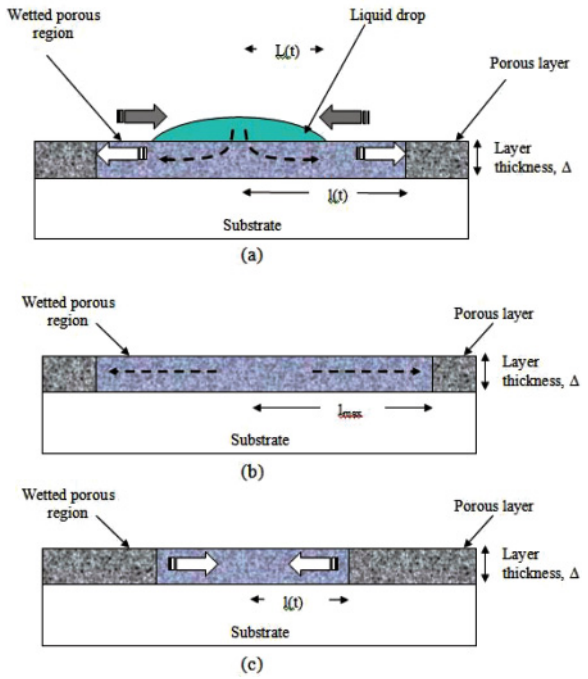

FIG. 3. (Color) Cross-sectional illustration of the thin porous layer during (a) first phase: shrinking of liquid drop and expansion of wetted porous region; (b) second phase: contact line pinning of wetted porous region with $l(t)$ remained constant at l_m; (c) third phase: shrinking of wetted porous region.

of the second phase. During the second phase, the diameter of the wetted porous region is maintained or "pinned" at its boundary. The boundary between the wetted porous region and the surrounding dry porous layer has a higher evaporation rate compared to the body of the wetted porous region due to a larger liquid vapor gradient and additional evaporation from the boundary of the wetted porous region into the dry porous region. However, instead of receding, the loss of liquid volume due to higher evaporation rate at the boundary is replenished by the adjacent pores with higher liquid volume, which corresponds to higher local capillary pressure, through continuous capillary flow. The redistribution of liquid volume within the pores is due to the tendency of a porous medium to achieve equal capillary pressure within the wetted porous region as described by Darcy's law of fluid flow in pore structures [12]. The wetted porous region body acts as a liquid reservoir, supplying a volume of liquid to the boundary with higher evaporation rate. This phenomenon is supported by observation of a previous publication reporting on a dyed liquid drop spread in a porous layer [13]. This increase in dye color intensity at the wetted porous region periphery over time indicates that the dye molecules are carried to the periphery of the wetted porous region by liquid carrier transport. The pinning of the wetted porous region will be maintained until the total liquid volume in the wetted porous region reached a "threshold" where the capillary pressure gradient over the entire wetted porous region becomes zero. At this point, the remaining liquid in the porous layer has negligible mobility.

C. Third phase

The third phase of liquid spreading starts when the total liquid volume threshold is reached. The wetted porous region will no longer be able to maintain its boundary. In this case, the liquid-filled pore fraction is uniform across the wetted porous region, and there is no fluid flow within the wetted porous region due to the lack of capillary pressure difference. Although the evaporation profile of the wetted porous region changes with the shrinking wetted region diameter, the relative evaporation rate at the boundary remains higher. This results in the residing of the wetted porous region boundary and the wetted porous region shrinks in the inward direction until the end of the process.

V. MODEL

Based on the description above, a model of evaporative liquid drop spreading dynamics on a thin porous layer is constructed. We first consider a scenario where a drop of nonevaporative liquid is applied onto a porous layer. While imbibition of a portion of the liquid into the porous medium takes place, the remaining portion of the liquid is left on top of the porous layer in a half-spherical shape drop. The total volume V_T of the liquid drop is given by

$$V_T(t) = V_{\text{res}}(t) + V_{\text{wet}}(t), \tag{1}$$

where $V_{\text{res}}(t)$ and $V_{\text{wet}}(t)$ are the liquid volume in the drop and porous medium, respectively. The total volume of the liquid drop remains unchanged over time, $\frac{dV_T}{dt} = 0$. Therefore, the liquid flow rates between the two mediums can be related by

$$\frac{dV_{\text{res}}}{dt} + \frac{dV_{\text{wet}}}{dt} = 0. \tag{2}$$

On the other hand, if an evaporative liquid is considered in this system, the rate of evaporation needs to be incorporated. The relation can be expressed by the partial differential equation (PDE) below:

$$\frac{dV_T}{dt} = \left(\frac{dV_S}{dt} + \frac{dV_{\text{wet}}}{dt}\right) - \frac{dV_{\text{eva}}}{dt}, \tag{3}$$

where $\frac{dV_{\text{eva}}}{dt}$ is the total evaporation rate from the liquid drop and wetted porous region. $V_S(t)$ in this case acts as a liquid source that supplies liquid volume to the expansion of the wetted porous region in the first phase and is responsible for the pinning of the wetted porous region boundary in the second phase. The variation of $V_S(t)$ can be described by the differential equation below:

$$\frac{dV_S}{dt} = -\alpha(V_S + \eta); \quad \alpha, \eta > 0, \tag{4}$$

where α is the supply rate constant and η describes the supply behavior. The liquid supply rate is linearly proportional to the time-dependent volume of the reservoir. Other environmental factors influencing the supply rate such as atmospheric pressure and capillary pressure are represented by η. Solving Eq. (4), we obtain

$$V_S(t) = (V_{S,0} + \eta)\exp(-\alpha t) - \eta, \tag{5}$$

where $V_{S,0}$ is the initial volume of the source. The outward liquid supply from the reservoir to the boundary stops when

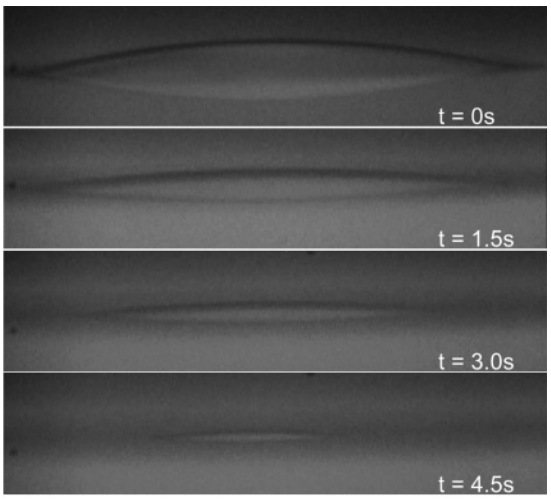

FIG. 4. Liquid drop profile evolution of a 1-μl DI water drop. Imbibition of liquid drop into the porous layer is completed in less than 5 s.

the capillary pressure gradient in the wetted porous region becomes zero. The source is then said to have reached depletion $V_S(t_r) = 0$ which occurs at the end of the second phase with the time given by

$$t_r = \frac{1}{\alpha} \ln\left(1 + \frac{V_{S,0}}{\eta}\right), \tag{6}$$

where t_r can be determined experimentally. To express the volume rate of change of the source as a function of time, we have

$$\frac{dV_S}{dt} = -\alpha S \exp(-\alpha t), \tag{7}$$

where $S = V_{S,0} + \eta$ is a lumped parameter for source volume change rate and $0 < t < t_r$. From experiments, the variation of total liquid volume V_T can be represented rather accurately by the characteristic equation below:

$$V_T(t) = \frac{k}{B} \ln\{1 + \exp[B(t_z - t)]\} + V_\infty, \tag{8}$$

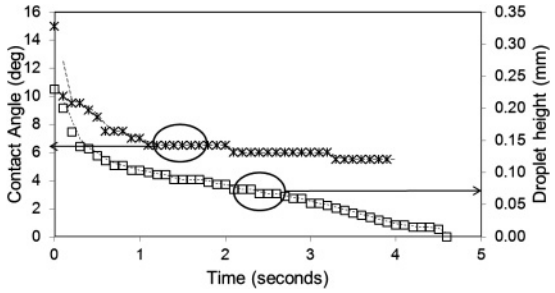

FIG. 5. Contact angle and liquid drop height as functions of time. The maximum height of the liquid drop is 0.23 mm. Contact angle is maintained at ~6° after decreasing from the initial value of 15° in the first second. Contact angle cannot be determined after 4 s as the liquid drop is too small.

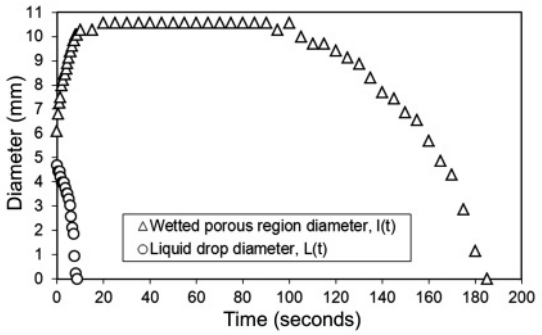

FIG. 6. Temporal development of liquid drop and wetted porous region diameter. Liquid drop volume used is 1.6 μl. The imbibition of liquid drop into the porous layer is completed in less than 9 s while time taken for the wetted porous region to disappear is 185 s.

where k, $B > 0$; $t_z = \frac{V_{T,0} - V_{T,\infty}}{k}$. Differentiating Eq. (8), we obtain the total volume loss rate:

$$\frac{dV_T}{dt} = -\frac{k}{1 + \exp[B(t - t_z)]}, \tag{9}$$

where k is the slope of the linear rate of total volume loss, obtained experimentally, and B is the characteristic coefficient. $V_{T,0}$ and $V_{T,\infty}$ denote the initial total volume and residue liquid volume in the system at the end of the spreading process. When

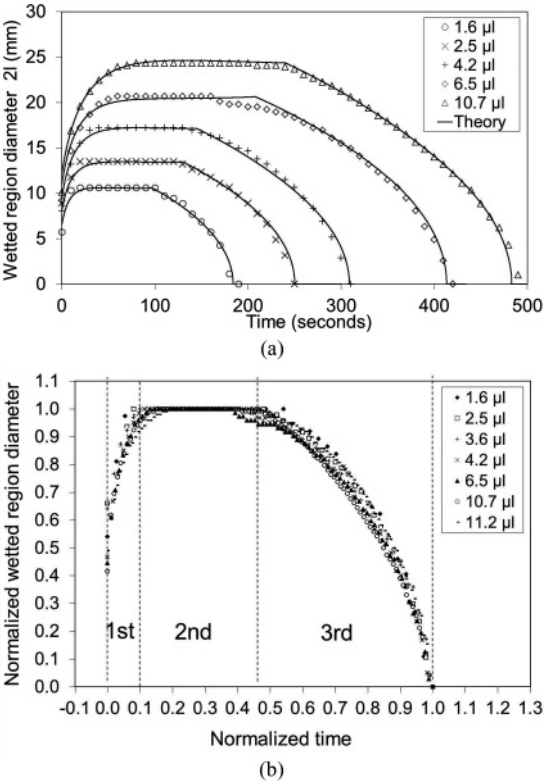

FIG. 7. (a) Temporal development of wetted porous region diameter with different initial liquid drop volume—both experimental and calculated data are fitted. (b) Normalized spreading diameter of wetted porous region over time for different initial liquid drop volume. The spreading diameter is normalized by the maximum diameter and the time by the final time, t_f.

a liquid drop is applied onto a thin porous layer, the portion of liquid that imbibes into the porous layer forms a wetted region in a shape of a cylindrical disk of radius l, thickness Δ, and porosity m. The liquid volume in the wetted region is given by

$$V_{\text{wet}} = m\Delta\pi l^2. \tag{10}$$

From visual observation of the wetted porous region, the boundary exhibits an effect that indicates a lower liquid-filled pore fraction. In this case, the actual V_{wet} is smaller. Therefore, the volume of liquid contained in the wetted region should be represented by

$$V_{\text{wet}} = mf\Delta\pi l^2, \tag{11}$$

where f is liquid-soot factor with values from 0 to 1 and is a function of maximum wetted region radius l_m.

The rate of change of V_{wet} is

$$\frac{dV_{\text{wet}}}{dt} = 2mf\Delta\pi l\frac{dl}{dt}. \tag{12}$$

The total evaporation rate is represented by

$$\frac{dV_{\text{eva}}}{dt} = J_0\pi l^2/\rho, \tag{13}$$

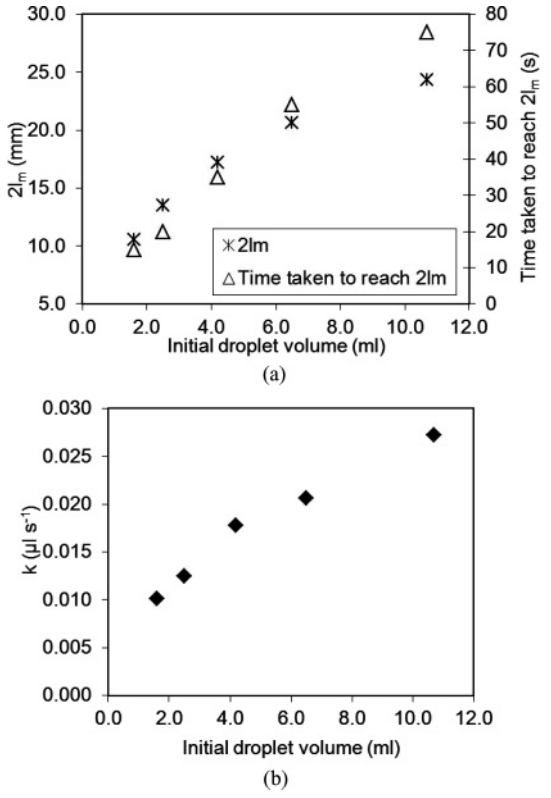

FIG. 8. (a) Maximum diameter of wetted region $2l_m$ and time taken to reach maximum diameter as a function of initial drop volume. (b) k is the total volume loss rate and is a function of initial drop volume.

where J_0 is the evaporation flux coefficient (evaporation rate per unit area) and ρ is the density of the liquid. Substitution of Eqs. (7), (9), (12), and (13) into Eq. (3) produces

$$-\alpha S\exp(-\alpha t) + 2mf\Delta\pi l\frac{dl}{dt} - \frac{J_0\pi}{\rho}l^2 = -\frac{k}{1+\exp[B(t-t_z)]}, \tag{14}$$

$$2l\frac{dl}{dt} - \frac{J_0}{\rho mf\Delta}l^2 = \frac{\alpha S}{\pi mf\Delta}\exp(-\alpha t) - \frac{k/\pi mf\Delta}{1+\exp[B(t-t_z)]}. \tag{15}$$

Solving Eq. (15), we obtain the function of the wetted porous region radius:

$$l^2(t) = \begin{cases} l^2(0)\exp(\gamma t) \\ +\frac{\alpha S[\exp(\gamma t)-\exp(-\alpha t)]}{\pi mf\Delta(\alpha+\gamma)} \\ -\frac{k\exp(\gamma t)}{\pi mf\Delta}\int_{\tau=0}^{\tau=t}\frac{\exp(-\gamma\tau)d\tau}{1+\exp[B(\tau-t_z)]}, & 0 \leqslant t \leqslant t_r \\ l^2(0)\exp(\gamma t) \\ +\frac{\alpha S[\exp(\gamma t_r)-\exp(-\alpha t_r)]}{\pi mf\Delta(\alpha+\gamma)} \\ -\frac{k\exp(\gamma t)}{\pi mf\Delta}\int_{\tau=0}^{\tau=t}\frac{\exp(-\gamma\tau)d\tau}{1+\exp[B(\tau-t_z)]}, & t_r < t \leqslant t_f \end{cases} \tag{16}$$

where $\gamma = J_0/\rho mf\Delta$ and $l(0)$ is assumed to be $0.5l_m$.

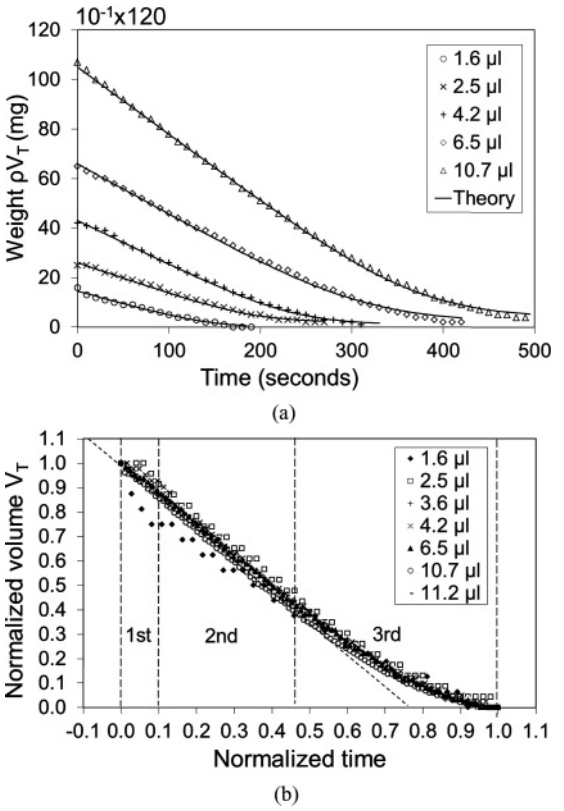

FIG. 9. (a) Change of liquid volume over time with different applied drop volume. (b) Normalized volume change over time for different applied liquid drop volume.

TABLE I. Details of the three spreading process phases.

Phase	Process description	Fraction of total process time	Evaporation rate
First	Wetted porous region formation	0.1	Constant
Second	Halt of expansion and constant wetted porous region size	0.4	Constant
Third	Shrinkage of wetted porous region	0.5	Reducing; zero when process ends

VI. RESULTS AND DISCUSSIONS

A. Development of wetted porous region diameter over time

Figure 4 shows the liquid drop profile evolution when a DI water drop with volume of 1.0 μl is applied on the thin porous layer. It is observed that the liquid drop reached maximum diameter almost instantly followed by a rapid shrink and disappeared in less than 5 s after the application of the liquid drop. Figure 5 shows measured liquid drop height and contact angle for the same liquid volume applied. Initial liquid drop height is 0.23 mm. Contact angle decreases from 15° to 6° in the first second and then maintain its angle at ~6° before total imbibition of the liquid drop into the porous layer.

A comparison of time evolution for the liquid drop profile and wetted porous region is shown in Fig. 6. The liquid drop volume used is 1.6 μl. The time taken for complete imbibition of the liquid drop into the porous layer is less than 9 s while the time taken for the wetted porous region to disappear is about 185 s. It can also be seen that the liquid drop reached its maximum diameter upon contact with the porous layer surface.

The diameter of the wetted porous region over time was recorded and plotted in Fig. 7(a). The wetted porous region diameter was measured in 5-s intervals. The volumes of DI water applied were 1.6, 2.5, 4.2, 6.5, and 10.7 μl. The change in diameter of the wetted porous region can be separated into three stages corresponding to the three phases discussed in Sec. III. The duration for each process phase became longer when a larger volume of liquid drop was applied. The maximum diameter also increases with larger DI water drop volume.

It is found that the ratio in duration between the three process phases is almost the same regardless of the initial drop volume V_T applied. This can be seen when the spreading profile of different liquid drop volumes is normalized by the maximum diameter of the wetted region, $2l_m$. Figure 7(b) shows the normalized spreading diameter of the wetted porous region when different volumes of DI water were applied. It can be seen that the spreading profile for different liquid drop volumes follows the same trend. The duration of the three phases of the spreading process can then be obtained as a fraction of the total spreading process duration. The first phase of the process where the formation of the wetted porous region takes place ends at about 10% into the total process duration t_f. The second process phase where the wetted porous region maintains its size occurs for about 40% of the total process duration, while the final 50% of the process duration involves the shrinkage of the wetted porous region. Using this time fraction, spreading profiles of different drop volumes are calculated and fitted in Fig. 7(a) using Eq. (16). Both experimental and calculated results show good agreement.

The relationship between the applied liquid drop volume and the resulting maximum wetted porous region diameter is shown in Fig. 8(a). The wetted porous region diameter ranges from 10.5 mm to 24.3 mm for a liquid volume of 1.6 μl and 10.7 μl, respectively. The same figure indicates that the time taken to reach maximum wetted porous region diameter increases with larger liquid drop volume. Therefore, the larger amount of liquid drop volume was lost through evaporation and resulted in a larger decrease from the initial drop volume when the maximum wetted region was reached. Another contributing factor to higher evaporation is the increased surface area of larger liquid drop volume for evaporation to

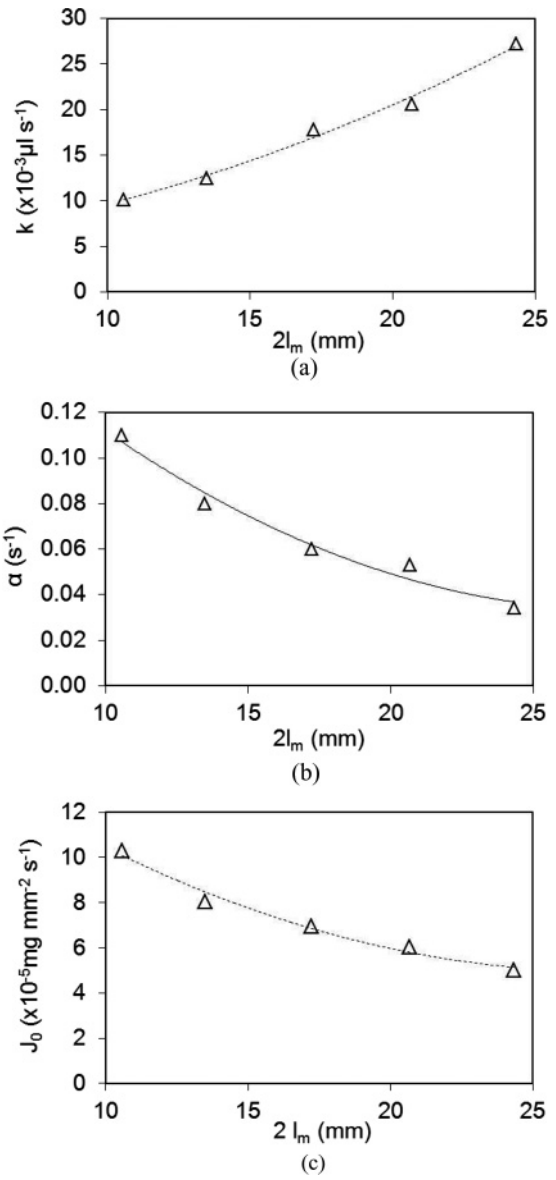

FIG. 10. Total volume loss rate k, supply rate constant α, and evaporation flux coefficient J_0 as functions of maximum wetted porous region diameter.

TABLE II. Summary of experimental and calculated results. $\rho = 1$ mg/mm^3, $\Delta = 25\times10^{-3}$mm, and $m = 0.8$.

Experimental results					Calculated results					
$V_{T,0}$ (mm^3)	t_r (s)	t_f (s)	k (mm^3 s^{-1})	l_m (mm)	S (mm^3)	f	α (s^{-1})	J_0 $\times10^{-5}$ (mg mm^{-2} s^{-1})	B ($\times10^{-3}$ s^{-1})	$J_0 l_m$ $\times10^{-4}$ (mg mm^{-1} s^{-1})
1.6	97	184	0.0101	5.28	0.82	0.661	0.110	10.31	35.0	5.44
2.5	130	250	0.0125	6.75	1.45	0.706	0.080	8.05	29.0	5.43
4.2	145	308	0.0178	8.60	3.00	0.826	0.060	6.94	25.5	5.97
6.5	208	405	0.0206	10.20	4.50	0.890	0.050	6.05	17.0	6.17
10.7	240	483	0.0272	12.16	8.20	1.000	0.034	5.00	18.6	6.08

take place. Figure 8(b) depicts the relationship between k and the drop volume.

B. Development of liquid drop volume over time

The change in liquid drop mass over time, implying the decrease in liquid drop volume within the wetted porous region, is depicted in Fig. 9(a). Loss of liquid drop volume is purely due to evaporation. The larger volume of liquid drop took a longer time for complete evaporation from the porous layer. No change of evaporation rate was observed from the start of the process up until the end of the second process phase. In the final phase of the process, the evaporation rate decreased, possibly due to shrinking of the wetted porous region. It was also observed that for larger drop volume, the weight of the sample did not return to zero at the end of the process when the wetted porous region is no longer observable. The remaining weight $\rho V_{T,\infty}$ is attributed to adsorbed liquid on the wall of the porous layer and is a function of the porous layer surface area exposed to the liquid during the spreading process. An attempt to quantify this relationship was made but the measurement is limited by the resolution of the digital analytical balance.

The normalized volume change rate of liquid drop during the spreading process is shown in Fig. 9(b). Again, the volume change rate for different liquid drop volumes shows good overlapping except for the applied liquid drop volume of 1.6 μl. The deviation is believed to be caused by larger measurement errors as a result of the resolution limit of the digital analytical balance. There is no observable change in the rate of volume loss or evaporation rate from the first process phase to the second process phase. However, the evaporation rate starts to decrease at about 50% into the total spreading process duration, which corresponds to the onset of the third phase—the shrinkage of the wetted porous region. Using Eq. (8), calculated results for total volume rate of change are fitted into Fig. 9(a). Again, both calculated and experimental results show good agreement with one another. The details of the three process phases are summarized in Table I.

The relationship between k, α, and J_0 with the maximum diameter $2l_m$ of the wetted porous region is shown in Fig. 10. k was measured during the second phase of the spreading process where the maximum diameter of the wetted porous region is maintained. It is observed that k increased linearly with the wetted porous region diameter, with values ranging from 10.1 μl/s to 27.2 μl/s for wetted porous region diameters of 10.6 mm and 24.3 mm, respectively. From the best-fit curves, α and J_0 are obtained and plotted in Figs. 10(b) and 10(c), respectively. It can be seen that α is inversely proportional to the maximum wetted porous region diameter. α decreases from 0.110 s^{-1} to 0.034 s^{-1} as the wetted region diameter increases from10.6 mm and 24.3 mm. The same trend is observed for J_o where the value decreases from 10.3×10^{-5} mg mm^{-2}·s^{-1} to 5×10^{-5} mg mm^{-2} s^{-1}.

Experimental and calculated results obtained are summarized in Table II. The total evaporation rate is in linear relation with the wetted porous region radius [2]:

$$J_0(\text{area}) \propto l. \tag{17}$$

Substituting area $= \pi l^2$, we have

$$J_0 \propto \frac{1}{l}. \tag{18}$$

In the scenario of varying wetted region radius, the maximum wetted porous region radius l_m is assumed:

$$J_0 \propto \frac{1}{l_m}. \tag{19}$$

This relationship is justified by the almost constant values of $J_0 l_m$ in the last column of Table II.

VII. CONCLUSION

Spreading of an evaporative liquid drop on a thin porous layer has been studied experimentally. The spread diameter and evaporation rate of a liquid drop in a porous layer with different drop volumes over time have been obtained. The spreading of the liquid drop into the porous layer can be divided into three phases, each occupying a different fraction of the total spreading time. It is observed that, regardless of the initial drop volume applied, spreading of the liquid drop for each of the three process phases follow relatively the same time intervals. Based on experimental observations, a model for liquid drop spreading of an evaporative liquid on a thin porous layer has been constructed. Results from both experiment and calculation agree well with each other, though the accuracy of the model can be further improved by considering other physical parameters such as viscosity of the liquid, adsorption and/or desorption of liquid with the porous layer surface, ambient humidity and temperature, etc. This study serves as a fundamental basis to predict fluid flow, spreading, and particle distribution in a thin porous layer for an evaporative liquid drop.

ACKNOWLEDGMENT

The authors would like to thank the University of Malaya for their High Impact Research Grant (UM.C/625/1/HIR/071) for partly supporting this work.

[1] R. D. Deegan, O. Bakajin, T. F. Dupont, G. Huber, S. R. Nagel, and T. A. Witten, Nature **389**, 827 (1997).
[2] R. D. Deegan, O. Bakajin, T. F. Dupont, G. Huber, S. R. Nagel, and T. A. Witten, Phys. Rev. E **62**, 756 (2000).
[3] V. M. Starov, S. R. Kosvintsev, V. D. Sobolev, M. G. Velarde, and S. A. Zhdanov, J. Colloid Interface Sci. **246**, 372 (2002).
[4] V. M. Starov, S. R. Kostvintsev, V. D. Sobolev, M. G. Velarde, and S. A. Zhdanov, J. Colloid Interface Sci. **252**, 397 (2002).
[5] V. M. Starov, S. A. Zhdanov, S. R. Kosvintsev, V. D. Sobolev, and M. G. Velarde, Adv. Colloid Interface Sci. **104**, 123 (2003).
[6] V. M. Starov, Adv. Colloid Interface Sci. **111**, 3 (2004).
[7] N. Shokri, P. Lehmann, and D. Or, J. Geophys. Res. **115**, B06204 (2010).
[8] N. Shokri, P. Lehmann, and D. Or, Phys. Rev. E **81**, 046308 (2010).
[9] M. Bechtold, S. Haber-Pohlmeier, J. Vanderborght, A. Pohlmeier, T. P. A. Ferre, and H. Vereecken, Geophys. Res. Lett. **38**, L17404 (2011).
[10] N. Shokri, P. Lehmann, P. Vontobel, and D. Or, Water Resour. Res. **44**, W06418 (2008).
[11] D. Banninger, P. Lehmann, H. Fluhler, and J. Toelke, Vadoze Zone Journal **4**, 1152 (2005).
[12] S. Whitaker, Transp. Porous Media **1**, 3 (1986).
[13] W. C. Leong, S. Y. Tho, A. W. P. Law, W. Y. Chong, C. H. Pua, H. Ahmad, A. S. M. A. Haseeb, and F. R. Mahamd Adikan, Thin Solid Films **518**, 378 (2009).